2007

A Robust Structural PGN Model for Control of Cell-Cycle Progression Stabilized by Negative Feedbacks

Hindawi Publishing Corporation
EURASIP Journal on Bioinformatics and Systems Biology
Volume 2007, Article ID 73109, 11 pages
doi:10.1155/2007/73109

Research Article

A Robust Structural PGN Model for Control of Cell-Cycle Progression Stabilized by Negative Feedbacks

Nestor Walter Trepode,[1] Hugo Aguirre Armelin,[2] Michael Bittner,[3] Junior Barrera,[1] Marco Dimas Gubitoso,[1] and Ronaldo Fumio Hashimoto[1]

[1] *Institute of Mathematics and Statistics, University of São Paulo, Rua do Matao 1010, 05508-090 São Paulo, SP, Brazil*
[2] *Institute of Chemistry, University of São Paulo, Avenue Professor Lineu Prestes 748, 05508-900 São Paulo, SP, Brazil*
[3] *Translational Genomics Research Institute, 445 N. Fifth Street, Phoenix, AZ 85004, USA*

Received 27 July 2006; Revised 24 November 2006; Accepted 10 March 2007

Recommended by Tatsuya Akutsu

The cell division cycle comprises a sequence of phenomena controlled by a stable and robust genetic network. We applied a probabilistic genetic network (PGN) to construct a hypothetical model with a dynamical behavior displaying the degree of robustness typical of the biological cell cycle. The structure of our PGN model was inspired in well-established biological facts such as the existence of integrator subsystems, negative and positive feedback loops, and redundant signaling pathways. Our model represents genes interactions as stochastic processes and presents strong robustness in the presence of moderate noise and parameters fluctuations. A recently published deterministic yeast cell-cycle model does not perform as well as our PGN model, even upon moderate noise conditions. In addition, self stimulatory mechanisms can give our PGN model the possibility of having a pacemaker activity similar to the observed in the oscillatory embryonic cell cycle.

1. INTRODUCTION

A complex genetic network is the central controller of the cell-cycle process, by which a cell grows, replicates its genetic material, and divides into two daughter cells. The cell-cycle control system shows adaptability to specific environmental conditions or cell types, exhibits stability in the presence of variable excitation, is robust to parameter fluctuation and is fault tolerant due to replications of network structures. It also receives information from the processes being regulated and is able to arrest the cell cycle at specific "*checkpoints*" if some events have not been correctly completed. This is achieved by means of intracellular *negative feedback* signals [1, 2].

Recently, two models were proposed to describe this control system. After exhaustive literature studies, Li et al. proposed a deterministic discrete binary model of the yeast cell-cycle control system, completely based on documented data [3]. They studied the signal wave generated by the model, that goes through all the consecutive phases of the cell-cycle progression, and verified, by simulation, that almost all the state transitions of this deterministic model converge to this "biological pathway," showing stability under different activation signal waveforms. Based on experimental data, Pomerening et al. proposed a continuous deterministic model for the self-stimulated embryonic cell-cycle, which performs one division after the other, without the need of external stimuli nor waiting to grow [4].

We recently proposed the probabilistic genetic network (PGN) model, where the influence between genes is represented by a stochastic process. A PGN is a particular family of Markov Chains with some additional properties (axioms) inspired in biological phenomena. Some of the implications of these axioms are: stationarity; all states are reachable; one variable's transition is conditionally independent of the other variables' transitions; the probability of the most probable state trajectory is much higher than the probabilities of the other possible trajectories (i.e., the system is almost deterministic); a gene is seen as a nonlinear stochastic gate whose expression depends on a linear combination of activator and inhibitory signals and the system is built by compiling these elementary gates. This model was successfully applied for designing malaria parasite genetic networks [5, 6].

Here we propose a hypothetical structural PGN model for the eukaryote control of cell-cycle progression, that aims

to reproduce the typical robustness observed in the dynamical behavior of biological systems. Control structures inspired in well-known biological facts, such as the existence of integrators, negative and positive feedbacks, and biological redundancies, were included in the model architecture. After adjusting its parameters heuristically, the model was able to represent dynamical properties of real biological systems, such as sequential propagation of gene expression waves, stability in the presence of variable excitation and robustness in the presence of noise [7].

We carried out extensive simulations—under different stimulus and noise conditions—in order to analyze stability and robustness in our proposed model. We also analyzed the performance of the yeast cell cycle control model constructed by Li et al. [3] under similar simulations. Under small noisy conditions, our PGN model exhibited remarkable robustness whereas Li's yeast-model did not perform that well. We infer that our PGN model very likely possesses some structural features ensuring robustness which Li's model lacks. To further emulate cellular environment conditions, we extended our model to include random delays in its regulatory signals without degrading its previous stability and robustness. Finally, with the addition of positive feedback, our model became self-stimulated, showing an oscillatory behavior similar to the one displayed by the embryonic cell-cycle [4]. Besides being able to represent the observed behavior of the other two models, our PGN model showed strong robustness to system parameter fluctuation. The dynamical structure of the proposed model is composed of: (i) prediction by an almost deterministic stochastic rule (i.e., gene model), and (ii) stochastic choice of an almost deterministic stochastic prediction rule (i.e., random delays).

After this introduction, in Section 2, we present our mathematical modeling of a gene regulatory network by a PGN. In Section 3, we briefly describe Li's yeast cell-cycle model and present the simulation, in the presence of noise, of our PGN version of it. Sections 4 and 5 describe the architecture and dynamics of our model for control of cell-cycle progression and analyze its simulations in the presence of noise and random delays in the regulatory signals (the same noise pattern was applied to both our model and Li's yeast-model). Section 6 shows the inclusion of positive feedback in our model to obtain a pacemaker activity, similar to the one found in embryonic cells. Finally, in Section 7 we discuss our results and the continuity of this research.

2. MATHEMATICAL MODELING OF GENETIC NETWORKS

2.1. Genetic regulatory networks

The cell cycle control system is a complex network comprising many forward and feedback signals acting at specific times. Figure 1 is a schematic representation of such a network, usually called a *gene regulatory network*. Proteins produced as a consequence of gene expression (i.e., after transcription and translation) form multiprotein complexes, that interact with each other, integrating extracellular signals—not shown—, regulating metabolic pathways (arrow 3), receiving (arrow 4) and sending (arrow 1 and 2) feedback signals. In this way, genes and their protein products form a signaling network that controls function, cell division cycle, and programmed cell death. In that network, the level of expression of each gene depends on both its own expression value and the expression values of other genes at previous instants of time, and on previous external stimuli. This kind of interactions between genes forms networks that may be very complex. The dynamical behavior of these networks can be adequately represented by discrete stochastic dynamical systems. In the following subsections, we present a model of this kind.

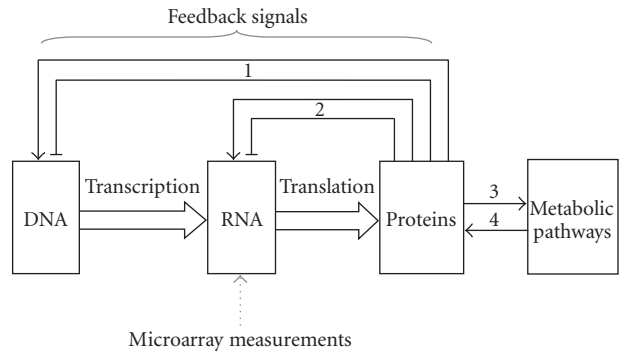

Figure 1: Gene regulatory network.

2.2. Discrete dynamical systems

Discrete dynamical systems, discrete in time and finite in range, can model the behavior of gene networks [8–12]. In this model, we represent each gene or protein by a variable which takes the value of the gene expression or the protein concentration. All these variables, taken collectively, are the components of a vector called the *state* of the system. Each component (i.e., gene or protein) of the state vector has associated a function that calculates its next value (i.e., expression value or protein concentration) from the state at previous instants of time. These functions are the components of a function vector, called *transition function*, that defines the transition from one state to the next and represents the actual regulatory mechanisms.

Let R be the range of all state components. For example, $R = \{0, 1\}$ in binary systems, $R = \{-1, 0, 1\}$ or $R = \{0, 1, 2\}$ in three levels systems. The transition function ϕ, for a network of N variables and *memory* m, is a function from R^{mN} to R^N. This means that the transition function ϕ maps the previous m states, $x(t-1), x(t-2), \ldots, x(t-m)$, into the state $x(t)$ with $x(t) = [x_1(t), x_2(t), \ldots, x_N(t)]^T \in R^N$. A discrete dynamical system is given by, for every time $t \geq 0$,

$$x(t) = \phi[x(t-1), x(t-2), \ldots, x(t-m)]. \quad (1)$$

A component of x is a value $x_i \in R$. Systems defined as above are time *translation invariant*, that is, the transition function is the same for all discrete time t. The system *architecture*—or structure—is the wiring diagram of the dependencies

between the variables (state vector components). The system *dynamics* is the temporal evolution of the state vector, given by the transition function.

2.3. Probabilistic genetic networks

When the transition function ϕ is a stochastic function (i.e., for each sequence of states $x(t-m),\ldots,x(t-2),x(t-1)$, the next state $x(t)$ is a realization of a random vector), the dynamical system is a stochastic process. Here we represent gene regulatory networks by stochastic processes, where the stochastic transition function is a particular family of Markov chains, that is called probabilistic genetic network (PGN).

Consider a sequence of random vectors $X_0, X_1, X_2, \ldots$ assuming values in R^N, denoted, respectively, $x(0), x(1)$, $x(2), \ldots$. A sequence of random states $(X_t)_{t=0}^{\infty}$ is called a *Markov chain* if for every $t \geq 1$,

$$\begin{aligned} P\big[X_t = x(t) \mid X_0 = x(0), \ldots, X_{t-1} = x(t-1)\big] \\ = P\big[X_t = x(t) \mid X_{t-1} = x(t-1)\big]. \end{aligned} \tag{2}$$

That is, the conditional probability of the future event, given the past history, depends only upon the last instant of time.

Let X, with realization x, represent the state before a transition, and let Y, with realization y be the first state after that transition. A Markov chain is characterized by a transition matrix $\pi_{Y|X}$ of conditional probabilities between states, whose elements are denoted $p_{y|x}$, and the probability distribution π_0 of the random vector representing the initial state. The stochastic transition function ϕ at time t, is given by, for every $t \geq 1$,

$$\phi[x] = \phi\big[x(t-1)\big] = y, \tag{3}$$

where y is a realization of a random vector with distribution $p_{\bullet|x}$.

An m order Markov chain—which depends on the m previous instants of time—is equivalent to a Markov chain whose states have dimension $m \times N$.

Let the sequence $\mathbf{X} = X_{t-1}, \ldots, X_{t-m}$ with realization $\mathbf{x} = x(t-1), \ldots, x(t-m)$ represent the sequence of m states before a transition. A *probabilistic genetic network* (PGN) is an m order Markov chain $(\pi_{Y|\mathbf{X}}, \pi_0)$ such that

(i) $\pi_{Y|\mathbf{X}}$ is homogeneous, that is, $p_{y|\mathbf{x}}$ is independent of t,

(ii) $p_{y|\mathbf{x}} > 0$ for all states $\mathbf{x} \in R^{mN}$, $y \in R^N$,

(iii) $\pi_{Y|\mathbf{X}}$ is conditionally independent, that is, for all states $\mathbf{x} \in R^{mN}$, $y \in R^N$,

$$p_{y|\mathbf{x}} = \Pi_{i=1}^{N} p(y_i \mid \mathbf{x}), \tag{4}$$

(iv) $\pi_{Y|\mathbf{X}}$ is almost deterministic, that is, for every sequence of states $\mathbf{x} \in R^{mN}$, there exists a state $y \in R^N$ such that $p_{y|\mathbf{x}} \approx 1$,

(v) for every variable i there exists a matrix a_i and a vector b_i of real numbers such that, for every $\mathbf{x}, \mathbf{z} \in R^{mN}$ and $y_i \in R$ if

$$\begin{aligned} \sum_{j=1}^{N} \sum_{k=1}^{m} a_{ji}^k x_j(t-k) = \sum_{j=1}^{N} \sum_{k=1}^{m} a_{ji}^k z_j(t-k), \\ \sum_{k=1}^{p_i} b_i^k x_i(t-k) = \sum_{k=1}^{p_i} b_i^k z_i(t-k), \\ \text{then } p(y_i \mid \mathbf{x}) = p(y_i \mid \mathbf{z}), \quad 0 \leq p_i \leq m. \end{aligned} \tag{5}$$

These axioms imply that each variable x_i is characterized by a matrix and a vector of coefficients and a stochastic function g_i from Z, a subset of integer numbers, to R.

If a_{ji}^k is positive, then the target variable x_i is *activated* by the variable x_j at time $t-k$, if a_{ji}^k is negative, then it is *inhibited* by variable x_j at time $t-k$, if a_{ji}^k is zero, then it is not affected by variable x_j at time $t-k$. We say that variable x_i is *predicted* by the variable x_j when some a_{ji}^k is different from zero. Similarly, if b_i^k is zero, the value of x_i at time t is not affected for its previous value at time $t-k$. The constant parameter p_i, for the state variable x_i, represents the number of previous instants of time at which the values of x_i can affect the value of $x_i(t)$. If $p_i = 0$, previous values of x_i have no effect on the value of $x_i(t)$ and the summation $\sum_{k=1}^{p_i} b_i^k x_i(t-k)$ is defined to be zero.

The component i of the stochastic transition function ϕ, denoted ϕ_i, is built by the composition of a stochastic function g_i with two linear combinations: (i) a_i and the previous states $x(t-1), \ldots, x(t-m)$, and (ii) b_i and the values of $x_i(t-1), \ldots, x_i(t-p_i)$. This means that, for every $t \geq 1$,

$$\phi_i\big[x(t-1), \ldots, x(t-m)\big] = g_i(\alpha, \beta), \tag{6}$$

where

$$\alpha = \sum_{j=1}^{N} \sum_{k=1}^{m} a_{ji}^k x_j(t-k), \qquad \beta = \sum_{k=1}^{p_i} b_i^k x_i(t-k) \tag{7}$$

and $g_i(\alpha, \beta)$ is a realization of a random variable in R, with distribution $p(\bullet \mid \alpha, \beta)$. This restriction on g_i means that the components of a PGN transition function vector are random variables with a probability distribution conditioned to two linear combinations, α and β, from the fifth PGN axiom.

The PGN model reflects the properties of a gene as a nonlinear stochastic gate. Systems are built by compiling these gates.

Biological rationale for PGN axioms

The axioms that define the PGN model are inspired by biological phenomena. The dynamical system structure is justified by the necessity of representing a sequential process. The discrete representation is sufficient since the interactions between genes and proteins occur at the molecular level [13]. The stochastic aspects represent perturbations or lack of detailed knowledge about the system dynamics. Axiom (i) is

just a constraint to simplify the model. In general, real systems are not homogeneous, but may be homogeneous by parts, that is, in time intervals. Axiom (ii) imposes that all states are reachable, that is, noise may lead the system to any state. It is a quite general model that reflects our lack of knowledge about the kind of noise that may affect the system. Axiom (iii) implies that the prediction of each gene can be computed independently of the prediction of the other genes, which is a kind of system decomposition consistent with what is observed in nature. Axiom (iv) means that the system has a main trajectory, that is, one that is much more probable than the others. Axiom (v) means that genes act as a nonlinear gate triggered by a balance between inhibitory and excitatory inputs, analogous to neurons.

3. YEAST CELL-CYCLE MODEL

The eukaryotic *cell-cycle* process is an ordered sequence of events by which the cell grows and divides in two daughter cells. It is organized in four *phases*: G_1 (the cell progressively grows and by the end of this phase becomes irreversibly committed to division), S (phase of DNA synthesis and chromosome replication), G_2 (bridging "gap" between S and M), and M (period of chromosomes separation and cell division) [1, 2]. The cell-cycle basic organization and control system have been highly conserved during evolution and are essentially the same in all eukaryotic cells, what makes more relevant the study of a simple organism, like yeast.

We made studies of stability and robustness on a recently published deterministic binary control model of the yeast cell-cycle, which was entirely built from real biological knowledge after extensive literature studies [3]. From the $\approx$ 800 genes involved in the yeast cell-cycle process [14], only a small number of key regulators, responsible for the control of the cell-cycle process, were selected to construct a model where each interaction between its variables is documented in the literature. A dynamic model of these interactions would involve various binding constants and rates [15, 16], but inspired by the on-off characteristic of many of the cell-cycle control network components, and focusing mainly on the overall dynamic properties and stability, they constructed a simple discrete binary model. In this work we refer to its simplified version, whose architecture is shown in Figure 1B of [3].

The simulation[1] in Figure 2(a) shows the state variables' temporal evolution over the biological pathway, that goes through all the sequential phases of the cell cycle, from the excited G_1 state (activated when CS—cell size—grows beyond a certain threshold), to the S phase, the G_2 phase, the M phase, and finally to the stationary G_1 state where it remains. The cell-cycle sequence has a total length of 13 discrete time steps (period of the cycle). Under simulations driven by CS pulses of increasing frequency,[2] this system behaved well, showing strong stability, with all initiated cycles systematically going to conclusion, and new cycles being initiated only after the previous one had finished.

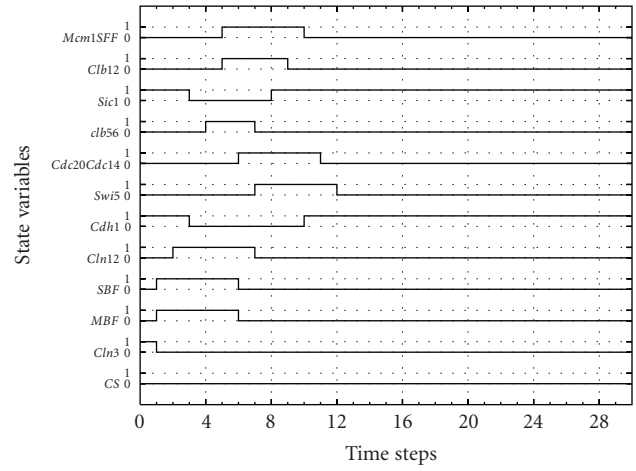

(a) Simulation of the deterministic binary yeast cell-cycle model with only one activator pulse of $CS = 1$ at $t = -1$. After the START state at $t = 0$, the system goes through the biological pathway, passing by all the sequential cell-cycle phases: G_1 at $t = 1, 2, 3$; S at $t = 4$; G_2 at $t = 5$; M at $t = 6, \ldots, 10$; G_1 at $t = 11$; and from $t = 12$ the system remains in the G_1 stationary state (all variables at zero level except $Sic1 = Cdh1 = 1$)

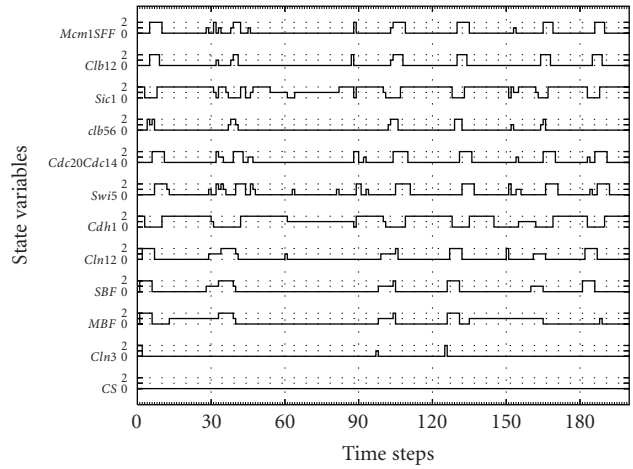

(b) Simulation of the three-level PGN yeast cell-cycle model with 1% of noise (PGN with $P = .99$) activated by a single pulse of $CS = 2$ at $t = -1$. After 13 time steps (period of the cycle), the system should remain in the G_1 stationary state—all variables at zero level except $Sic1 = Cdh1 = 2$—(compare with Figure 2(a)). Instead, this small amount of noise is enough to take the system completely out of its expected normal behavior

FIGURE 2: Yeast cell-cycle model simulations.

3.1. PGN yeast cell-cycle model

In order to study the effect of noise and the increase of the number of signal levels in the performance of Li's yeast-model [3], we translated it into a three level PGN model. Initially, we mapped Li's binary deterministic model into a three

[1] All simulations in this work were performed using SGEN (simulator for gene expression networks) [17].
[2] Simulations are not shown here.

Table 1: Threshold values for variables without self-degradation in the PGN yeast cell-cycle model.

	$x_i(t-1)=0$	$x_i(t-1)=1$	$x_i(t-1)=2$
$\text{th}_{x_i}^{(1)}$	1	0	-1
$\text{th}_{x_i}^{(2)}$	2	1	0

level deterministic one, with range of values $R = \{0, 1, 2\}$ for the state variables. By PGN axiom (iv), the PGN transition matrix $\pi_{Y|\mathbf{X}}$ is almost deterministic, that is, at every time step, one of the transition probabilities $p_{y|\mathbf{x}} \approx 1$. The deterministic case would be the case when, at every time step, this most probable transition have $p_{y|\mathbf{x}} \to 1$, or, in real terms, the case corresponding to total absence of noise in the system. In this mapping, binary value 1 was mapped to 2, and binary value 0 was mapped to 0, of the three-level model. Intermediate values (in the driving and transition functions) were mapped in a convenient way, so that they lay between the ones that have an exact correspondence. From this deterministic three-level model (having exactly the same dynamical behavior of the binary model from which it was derived) we specified the following PGN.

3.1.1. PGN specification and simulation

The total input signal driving a generic variable $x_i(t) \in \{0, 1, 2\}$ $(1 \le i \le N)$ is given by its associated *driving function*:

$$d_i(t-1) = \sum_{j=1}^{N} a_{ji} x_j(t-1). \tag{8}$$

Here, the system has *memory* $m = 1$ and a_{ji} is the weight for variable x_j at time $t-1$ in the driving function of variable x_i. If variable x_j is an activator of variable x_i, then $a_{ji} = 1$; if variable x_j is an inhibitor of variable x_j, then $a_{ji} = -1$; otherwise, $a_{ji} = 0$.

Let

$$y_i(t) = \begin{cases} 2 & \text{if } d_i(t-1) \ge \text{th}_{x_i}^{(2)}, \\ 1 & \text{if } \text{th}_{x_i}^{(1)} \le d_i(t-1) < \text{th}_{x_i}^{(2)}, \\ 0 & \text{if } d_i(t-1) < \text{th}_{x_i}^{(1)}. \end{cases} \tag{9}$$

The *stochastic transition function* chooses the next value of each variable to be (i) $x_i(t) = y_i(t)$ with probability $P \approx 1$, (ii) $x_i(t) = a$ with probability $(1-P)/2$, or (iii) $x_i(t) = b$ with probability $(1-P)/2$; where $a, b \in \{0, 1, 2\} - \{y_i\}$ and $\text{th}_{x_i}^{(1)}$, $\text{th}_{x_i}^{(2)}$ are the threshold values for one and two in the transition function of variable x_i. For this model to converge, when $P \to 1$, to the deterministic one in the previous subsection, these thresholds must have the values indicated in Table 1, depending on the value of $x_i(t-1)$. If variable x_i has the self degradation property, its threshold values are those in the column of $x_i(t-1) = 0$, regardless of the actual value of $x_i(t-1)$.

We simulated the three-level PGN version of Li's yeast-model with probability $P = 0.99$ to represent the presence of 1% of noise in the system. Figure 2(b) shows a 200 steps simulation of the system when the G_1 stationary state is activated by a single start pulse of $CS = 2$ at $t = -1$. Comparing with Figure 2(a), we observe that this moderate noise is sufficient to degrade the systems' performance. Particularly, the system should remain in the G_1 stationary state after the 13 steps cycle period, however, numerous spurious waveforms are generated. Furthermore, when we simulated this system increasing the frequency of the *CS* activator pulses, noise seriously disturbed the normal signal wave propagation [18]. We conclude that this system does not have a robust performance under 1% of noise.

4. OUR STRUCTURAL MODEL FOR CONTROL OF CELL-CYCLE PROGRESSION

The PGN was applied to construct a hypothetical model based on components and structural features found in biological systems (integrators, redundancy, positive forward signals, positive and negative feedback signals, etc.) having a dynamical behavior (waves of control signals, stability to changes in the input signal, robustness to some kinds of noise, etc.) similar to those observed in real cell-cycle control systems.

During cell-cycle progression, families of genes have either brief or sustained expression during specific cell-cycle phases or transitions between phases (see, e.g., Figure 7 in [14]). In mammalian cells, the transition G_0/G_1 of cell cycle requires sequential expression of genes encoding families of master transcription factors, for instance the fos and jun families of proto-oncogenes. Among the fos genes c-fos and fos B are essentially regulated at transcription level and are expressed for a brief period of time (0.5 to 1 h), displaying mRNAs and proteins of very short half life. In addition, G_1 progression and G_1/S transition are controlled by the cell cycle regulatory machine, comprised by proteins of sustained (cyclin-dependent kinases—CDKs—and Rb protein) and transient expression (cyclins D and E). The genes encoding cyclins D and E are transcribed at middle and late G_1 phase, respectively. Actually, there are several CDKs regulating progression along all cell cycle phases and transitions, whose activities are dependent on cyclins that are transiently expressed following a rigid sequential order. This basic regulation of cell cycle progression is highly conserved in eukaryotes, from yeast to mammalians. Accordingly, we organized our model into successive gene layers expressed sequentially in time. This wave of gene expression controls timing and progression through the cell-cycle process.

The architecture of our cell-cycle control model is depicted in Figure 3, showing the forward and feedback regulatory signals between gene layers (**s**, **T**, **v**, **w**, **x**, **y**, and **z**), that determine the system's dynamic behavior. These gene layers represent consecutive stages taking place along the classical cell-cycle phases G_1, S, G_2, and M. These layers are comprised by the genes—state variables—expressed during the execution of each stage and are grouped into the two main parts: (i) G_1 phase—layer **s**—that represents the cell growth phase immediately before the onset of DNA

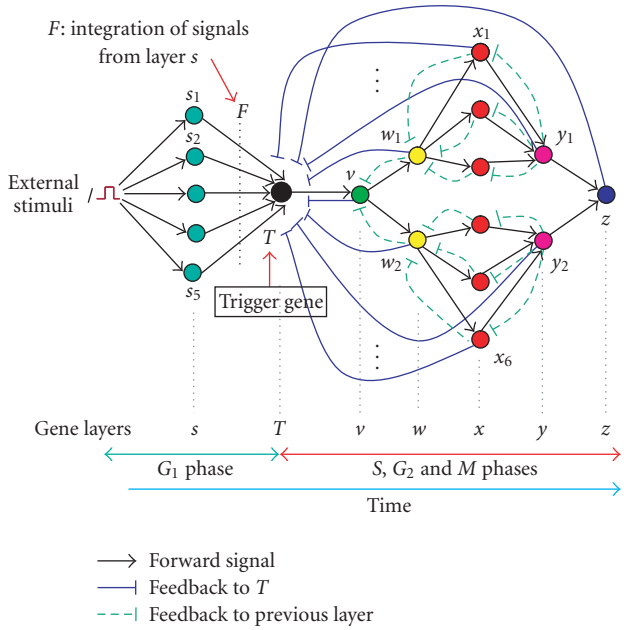

Figure 3: Cell-cycle network architecture.

replication (i.e., S phase), during which the cell responds to external regulatory stimuli (I) and (ii) S, G_2 plus M phases—layers **T**, **v**, **w**, **x**, **y**, and **z**—that goes from DNA replication to mitosis. The S phase trigger gene T represents an important cell-cycle checkpoint, interfacing G_1 phase regulatory signals and the initiation of DNA replication. The signal F (Figure 3) stands for integration, at the trigger gene T, of activator signals from layer **s**. Our basic assumption implies that the cell-cycle control system is comprised of modules of parallel sequential waves of gene expression (layers **s** to **z**) organized around a check-point (trigger gene T) that integrates forward and feedback signals. For example, within a module, the trigger gene T balances forward and feedback signals to avoid initiation of a new wave of gene expression while a first one is still going through the cell cycle. A number of check-point modules, across cell cycle, regulate cell growth and genome replication during the sequential G_1, S, and G_2 phases and cell duplication via mitosis.

In our model, the expression of one of the genes in layers **v** to **z** (i.e., after the trigger gene T—see Figure 3) typically yields three types of signals in the system: (i) a *forward activator signal* to genes in the *next layer* that tends to make the cell-cycle progress in its sequence; (ii) an *inhibitory feedback signal* to the genes in the *previous layer* aiming to stop the propagation of a new forward signal for some time; and (iii) an *inhibitory feedback signal* to the *trigger gene* T that tends to avoid the triggering of a new wave of gene expression while the current cycle is unfinished. The negative feedback signals perform an important regulatory action, tending to ensure that a new forward signal wave is not initiated nor propagated through the system when the previous one is still going on. This imposes in the model essential robustness features of the biological cell cycle, for example, a cycle must be completed before initiating another cycle of cell duplication and division. Parallel signaling also provide robustness, acting as backup mechanisms in case of parts malfunction.

Table 2: PGN weight values and transition function thresholds.

Weights	Thresholds
$a^k_{FP} = 6, k = 5, 6, \ldots, 9$ $a^1_{jP} = -2, j = v, w, x, y, z$	$\text{th}^{(1)}_P = 9, \text{th}^{(2)}_P = 12$
$a^k_{Pv} = 4, k = 5, 6, \ldots, 9$ $a^k_{wv} = -2, k = 1, 2$	$\text{th}^{(1)}_v = 11, \text{th}^{(2)}_v = 22$
$a^k_{vw} = 6, k = 5, 6, \ldots, 9$ $a^k_{xw} = -1, k = 1, 2$	$\text{th}^{(1)}_w = 20, \text{th}^{(2)}_w = 35$
$a^k_{wx} = 5, k = 5, 6, \ldots, 9$ $a^k_{yx} = -1, k = 1, 2$	$\text{th}^{(1)}_x = 20, \text{th}^{(2)}_x = 28$
$a^5_{xy} = 2$	$\text{th}^{(1)}_y = 6, \text{th}^{(2)}_y = 12$
$a^5_{yz} = 2$	$\text{th}^{(1)}_z = 4, \text{th}^{(2)}_z = 8$

4.1. Complete PGN specification

This PGN is specified in the same way as the one in Section 3.1.1, changing the *driving function* to the following:

$$d_i(t-1) = \sum_{j=1}^{N} \sum_{k=1}^{m} a^k_{ji} x_j(t-k), \tag{10}$$

where m is the *memory* of the system and a^k_{ji} is the weight for variable x_j at time $t-k$ in the driving function of variable x_i; and using the weight and threshold values shown in Table 2, where a^k_{ji} is the weight for the expression values of genes in layer j at time $t-k$ in the driving function at time t of genes at layer i. Weight values not shown in the table are zero. Thresholds are the same for all genes in the same layer.

4.2. Experimental results

We simulated our hypothetical cell-cycle control model, as a PGN with probability $P = .99$ driven by different excitation signals F (integration of signals from layer **s** driving the trigger gene T): beginning with a single activation pulse ($F = 2$), then pulses of F of increasing frequency—that is, pulses arriving each time more frequently in each simulation—and, finally, with a constant signal $F = 2$. As the initial condition for the simulations of our model, we chose all variables from layers **T** to **z** at zero value in the m—memory of the system—previous instants of time. This represents, in our model, the G_1 stationary state, where the system remains after a previous cycle has ended and when there is no activator signal F strong enough to commit the cell to division. For simplicity, when plotting these simulations, we show only one representative gene for each gene layer.

A single pulse of F (Figure 4(a)) makes the system go through all the cycle stages and then, all signals remain at

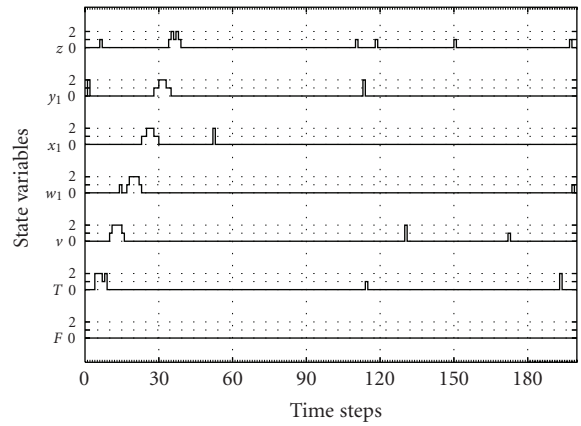

(a) One single start pulse of $F = 2$ at $t = -1$

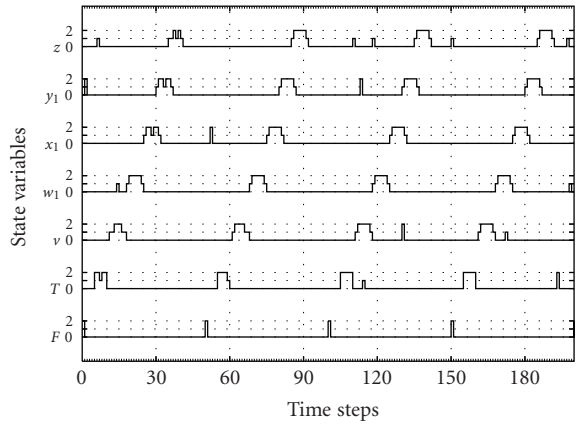

(b) F = Period 50 oscillator

Figure 4: Simulation of our three-level PGN cell-cycle progression control model with 1% of noise (PGN with $P = .99$) when activator pulses of F arrive after the previous cycle has ended.

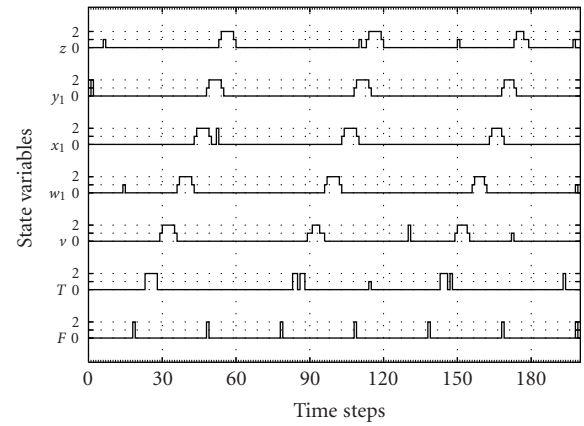

(a) F = period 30 oscillator

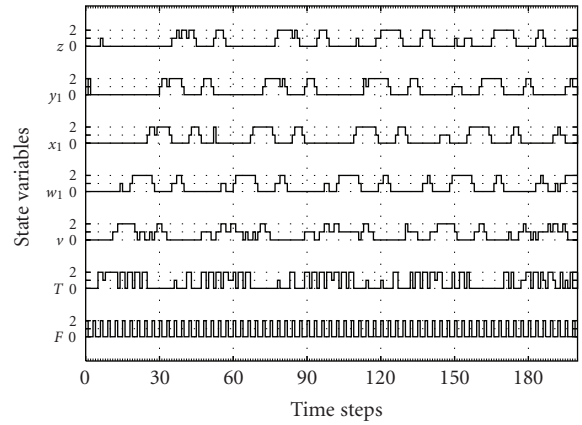

(b) F = period 3 oscillator

Figure 5: Simulation of our three level PGN cell-cycle progression control model with 1% of noise (PGN with $P = 0.99$) when activator pulses of F can arrive before the previous cycle has ended.

zero level—G_1 stationary state—with a very small amount of noise. Comparing this simulation with the one in Figure 2(b) (three-level PGN model of the yeast cell cycle under the same noise and activation conditions), we see that this system is almost unaffected by this amount of noise during the cycle progression or when it is in a stationary state. Those small extra pulses, that arise outside the signal trains in the simulations of our model, are the observable effect due to the presence of 1% of noise (they do not appear when the system is simulated without noise [19]—not shown here). Figure 4(b) shows that when new F activator pulses are applied *after* each cycle is finished, cycles start and are completed normally.

For F pulses arriving more frequently, a new cycle is started *only* if the previous one has finished (Figure 5(a)). This control action is performed by the inhibitory negative feedback signals—from layers **v** to **z**—acting on the trigger gene T, carrying the information that a previous cycle is still unfinished. We see, in these simulations, that no spurious signal waves are generated by noise nor the forward cell-cycle signal is stopped by it (i.e., all normally initiated cycles finish). If a very frequent train of pulses triggers gene T before the end of the ongoing cycle, that signal is stopped at the following gene layers by the negative interlayer feedbacks. The regulation performed by these interlayer feedbacks provide another timing effect, assigning each stage—or layer—a given amount of time for the processes it controls, stopping the propagation of a new forward signal wave—coming from the previous layer—for some time. By means of two types of negative feedbacks (to the previous layer and to gene T), this system is able to resist the excessive activation signal, maintaining its natural period, and thus mimicking the biological cell cycle in nature. But, as in biological systems robustness has its limits, in our model a very frequent excitation (short period train of F pulses—Figure 5(b)—or constant $F = 2$—not shown here) surpasses the resistance of the negative feedbacks, taking the system out of its normal behavior.

For comparison purposes, we simulated both Li's model and ours with 1% of noise. In other simulations, not shown here, we increased gradually the noise in our model to see how much it can resist, and decreased gradually the noise in Li's model to determine the smallest amount of it that can lead to undesired dynamical behavior. In the first case,

Table 3: Delay probabilities.

t_d	$P(t_d)$
0	.2
1	**.6**
2	.2

Table 4: PGN weight values and transition function thresholds in the model with random delays in the regulatory signals.

Weights ($k = k' + t_d$)	Thresholds
$a_{FT}^{k'} = 6, k' = 5, \ldots, 9$	$\text{th}_T^{(1)} = 9$
$a_{jT}^{k'} = -1.33; j = v, w, x, y, z; k' = 1$	$\text{th}_T^{(2)} = 12$
$a_{jT}^{k'} = -0.67; j = v, w, x, y, z; k' = 2$	—
$a_{Tv}^{k'} = 5, k' = 5, \ldots, 9$	$\text{th}_v^{(1)} = 11$
$a_{wv}^{k'} = -0.77, k' = 1, \ldots, 9$	$\text{th}_v^{(2)} = 22$
$a_{vw}^{k'} = 7, k' = 3, \ldots, 7$	$\text{th}_w^{(1)} = 15$
$a_{xw}^{k'} = -0.83, k' = 1, \ldots, 9$	$\text{th}_w^{(2)} = 25$
$a_{wx}^{k'} = 6, k' = 4, \ldots, 8$	$\text{th}_x^{(1)} = 20$
$a_{yx}^{k'} = -1.77, k' = 1, \ldots, 9$	$\text{th}_x^{(2)} = 28$
$a_{xy}^{k'} = 3, k' = 6$	$\text{th}_y^{(1)} = 6$
	$\text{th}_y^{(2)} = 12$
$a_{yz}^{k'} = 3, k' = 6$	$\text{th}_z^{(1)} = 4$
	$\text{th}_z^{(2)} = 8$

we observed that in our model, a noise above 3% is needed for a noise pulse to propagate through the consecutive layers as a spurious signal train (5% of noise is needed to stop the normal signal wave, preventing it from finishing an ongoing cell cycle) [19]. On the other hand, when simulating Li's binary model, we observed spurious pulse propagation even at 0.05% noise [18].

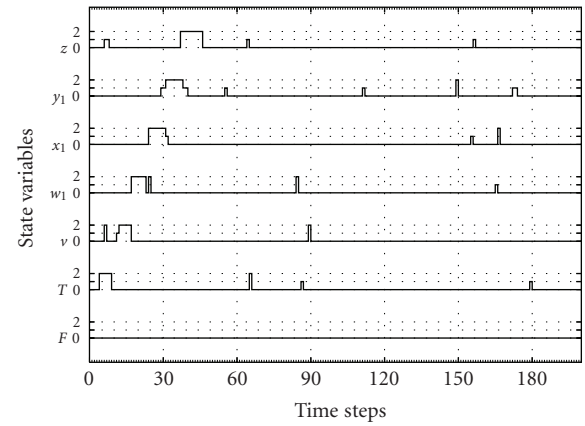

(a) One single start pulse of $F = 2$ at $t = -1, -2$

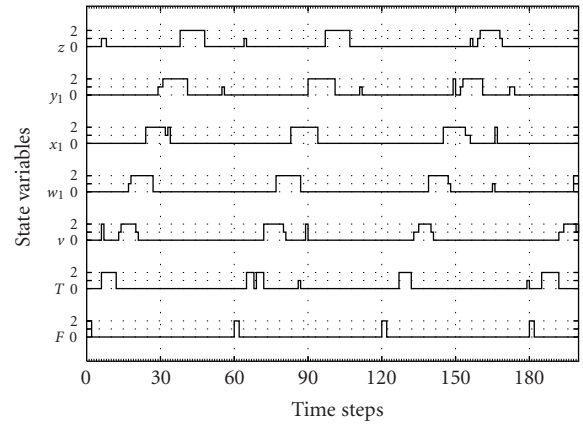

(b) F = period 60 oscillator

Figure 6: Simulation of our three-level PGN cell-cycle progression control model with random delays and 1% of noise (PGN with $P = .99$), when activator pulses of F arrive after the previous cycle has ended.

5. CELL-CYCLE PROGRESSION CONTROL MODEL WITH RANDOM DELAYS

We modified our model in order to admit random delays in signal propagation, maintaining its overall behavior and robustness.

5.1. PGN specification

In this version, before computing the driving function of a variable, the model chooses a random delay t_d for its arguments, with the probability distribution of Table 3. Once these delays are chosen, the stochastic transition function defined in Section 4.1 calculates the temporal evolution of the system, with the weights and thresholds indicated in Table 4. The transition function parameters, specifically its PGN weights values, depend on these variable delays. As shown in Table 4, these delays produce a time displacement of the weights, and so, of the inputs to the driving function of each variable. This system is no longer time translation invariant, but adaptive. At each time step, it chooses a PGN from a set of candidate PGNs (each one determined by one of the possible combinations of delays for its variables).

In Table 4, a_{ji}^k denotes the weight for the expression values of genes in layer j at time $t - k$ (where $k = k' + t_d$) in the driving function of layer i genes at time t. Weight values not shown in the table are zero. Thresholds are the same for all genes in the same layer, but t_d is not. It is chosen individually for each gene—by its associated component of the transition function—at each step of discrete time.

5.2. Experimental results

We simulated this new model—with random delays—in the same conditions as the previous one obtaining a similar dynamical behavior. Due to the random delays applied at every time step in the signals, the waveform widths and the period of the cycle are somewhat variable and longer than they were in the previous model.

Figure 6 shows the behavior of the system when it is driven by a single pulse of $F = 2$ or by a train of pulses whose

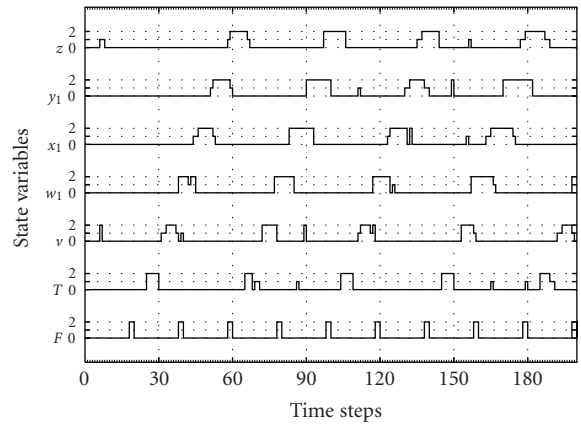

(a) F = period 20 oscillator

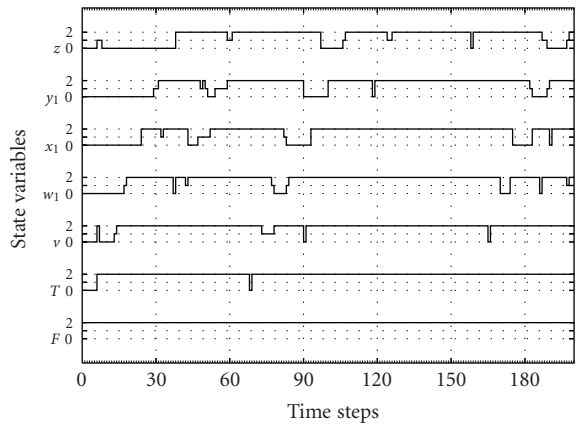

(b) Constant $F = 2$

FIGURE 7: Simulation of our three-level PGN cell-cycle progression control model with random delays and 1% of noise (PGN with $P = .99$), when activator pulses of F arrive before the previous cycle has ended, and with constant activation $F = 2$.

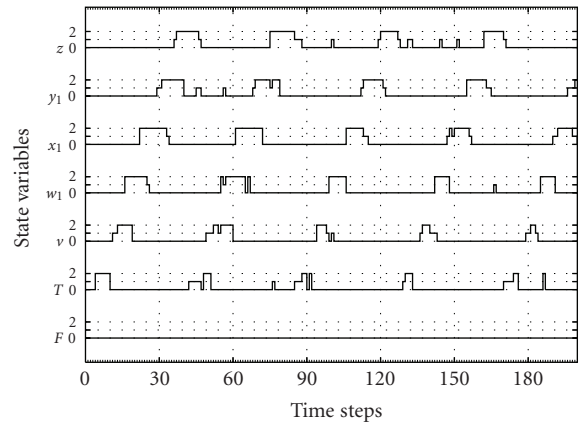

(a) Due to the positive feedback from z to T, a new cycle is started right after the previous one has finished, without the need of a new F activator signal. This behavior is typical of the embryonic cell-cycle, which depends on positive feedback loops to maintain undamped oscillations with the correct timing

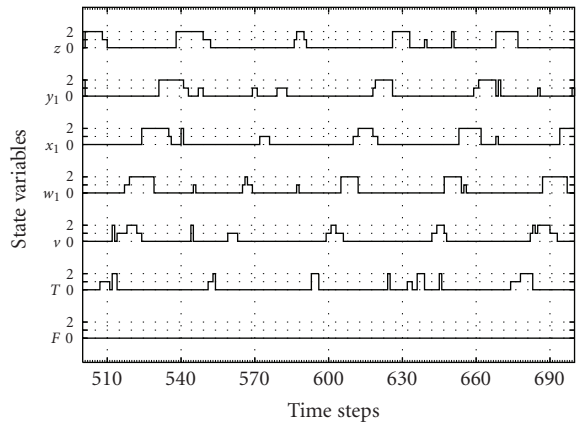

(b) The second cycle in this figure is somewhat weakened (by the effect of noise and random delays), but the positive feedback gets to overcome this (without the need of F activation) and the system recovers its normal cyclical activity

FIGURE 8: PGN cell-cycle progression control model with positive feedback from gene z to the trigger gene T ($a^k_{zT} = 7, k = 5 + t_d$), 1% of noise and only one initial activator pulse $F = 2$ at $t = -1, -2$.

period is greater than the cycle period. The system behaves normally, with a little amount of noise, much weaker than the regulatory signals. When F pulses arrive more frequently and the period of the activator signal is shorter than the period of the cycle (Figure 7(a)), a new cycle is not started if the activator pulse arrives when the previous cycle has not been completed. Finally, when the activation F becomes very frequent or constant (Figure 7(b)), the negative feedbacks can no longer exert their regulatory action and the system undergoes disregulation.

These simulations show the degree of robustness of our model system under noise and random delays, when driven by a wide variety of activator signals [20].

6. CELL-CYCLE PROGRESSION CONTROL MODEL WITH RANDOM DELAYS AND POSITIVE FEEDBACK

Our model can exhibit a pacemaker activity, initiating one-cell division cycle after the previous one has finished without the requirement of external stimuli, if we include positive feedback in it. This oscillatory behavior is observed in nature during proliferation of embryonic cells [4]. For our model to present this oscillatory behavior, it suffices to include a positive feedback signal from gene z—last layer—to the trigger gene T. The system is exactly the same as the previous random delay PGN model, except for an additional weight different of zero: $a^k_{zT} = 7$ (where $k = 5 + t_d$).

6.1. Experimental results

In the simulation of Figure 8, the system is initially driven by a single pulse of $F = 2$ at $t = -1, -2$. As in the embryonic cell cycle, the positive feedback loop induces a pacemaker activity

where all cycles are completed normally with the correct timing for all the different phases. A new cycle starts right after the completion of the previous one without the need of any activator signal F. Figure 8(b) shows that when a signal wave is weakened by the combined effect of noise and random delays, the positive feedback (without the need of any F activation) is sufficient to overcome this signal failure, putting the system back into a normal-amplitude cyclical activity. These simulations show the flexibility of our PGN model to represent different types of dynamical behavior, including the embryonic cell-cycle, that is induced by positive feedback loops.

7. DISCUSSION

We designed a PGN hypothetical model for control of cell-cycle progression, inspired on qualitative description of well-known biological phenomena: the cell cycle is a sequence of events triggered by a control signal that propagates as a wave; there are signal integrating subsystems and (positive and negative) feedback loops; parallel replicated structures make the cell-cycle control fault tolerant. Furthermore, important real-world nonbiological control systems usually are designed to be stable, robust, fault tolerant and admit small probabilistic parameter fluctuations.

Our model's parameters were adjusted guided by the expected behavior of the system and exhaustive simulation. This modeling effort had no intention of representing details of molecular mechanisms such as kinetics and thermodynamics of protein interactions, functioning of the transcription machinery, microRNA, and transcription factors regulation, but their concerted effects on the control of gene expression [13].

Our cell-cycle progression control model was able to represent some behavioral properties of the real biological system, such as: (i) sequential waves of gene expression; (ii) stability in the presence of variable excitation; (iii) robustness under noisy parameters: (iii-i) prediction by an almost deterministic stochastic rule; (iii-ii) stochastic choice of an almost deterministic stochastic prediction rule (random delays), and (iv) auto stimulation by means of positive feedback.

The presence of numerous negative feedback loops in the model provide stability and robustness. They warrant that, under multiple noisy perturbation patterns, the system is able to automatically correct external stimuli that could destroy the cell. This kind of mechanisms has commonly been found in nature. Particularly, we think that the robustness of Li's yeast cell-cycle model [3] would be improved by addition of critical negative feedback loops, that we suspect should exist in the biological system. The inclusion of positive feedback can make our model capable of exhibiting a pacemaker activity, like the one observed in embryonic cells. The parallel structure of the system architecture represents biological redundancy, which increases system fault tolerance.

Our discrete stochastic model qualitatively reproduces the behavior of both Li et al. [3] and Pomerening et al. [4] models, exhibiting remarkable robustness under noise and parameters' random variation. The natural follow up of this research is to infer the PGN model from available dynamical data of cell-cycle progression, analogously to what we have done for the regulatory system of the malaria parasite [5, 6]. We anticipate that, very likely, analysis of these dynamical data will uncover unknown negative feedback loops in cell-cycle control mechanisms.

ACKNOWLEDGMENTS

This work was partially supported by Grants 99/07390-0, 01/14115-7, 03/02717-8, and 05/00587-5 from FAPESP, Brazil, and by Grant 1 D43 TW07015-01 from The National Institutes of Health, USA.

REFERENCES

[1] A. Murray and T. Hunt, *The Cell Cycle*, Oxford University Press, New York, NY, USA, 1993.

[2] B. Alberts, A. Johnson, J. Lewis, M. Raff, K. Roberts, and P. Walter, *Molecular Biology of the Cell*, Garland Science, New York, NY, USA, 4th edition, 2002.

[3] F. Li, T. Long, Y. Lu, Q. Ouyang, and C. Tang, "The yeast cell-cycle network is robustly designed," *Proceedings of the National Academy of Sciences of the United States of America*, vol. 101, no. 14, pp. 4781–4786, 2004.

[4] J. R. Pomerening, S. Y. Kim, and J. E. Ferrell Jr., "Systems-level dissection of the cell-cycle oscillator: bypassing positive feedback produces damped oscillations," *Cell*, vol. 122, no. 4, pp. 565–578, 2005.

[5] J. Barrera, R. M. Cesar Jr., D. C. Martins Jr., et al., "A new annotation tool for malaria based on inference of probabilistic genetic networks," in *Proceedings of the 5th International Conference for the Critical Assessment of Microarray Data Analysis (CAMDA '04)*, pp. 36–40, Durham, NC, USA, November 2004.

[6] J. Barrera, R. M. Cesar Jr., D. C. Martins Jr., et al., "Constructing probabilistic genetic networks of plasmodium falciparum from dynamical expression signals of the intraerythrocytic developement cycle," in *Methods of Microarray Data Analysis V*, chapter 2, Springer, New York, NY, USA, 2007.

[7] N. W. Trepode, H. A. Armelin, M. Bittner, J. Barrera, M. D. Gubitoso, and R. F. Hashimoto, "Modeling cell-cycle regulation by discrete dynamical systems," in *Proceedings of IEEE Workshop on Genomic Signal Processing and Statistics (GENSIPS '05)*, Newport, RI, USA, May 2005.

[8] S. A. Kauffman, *The Origins of Order*, Oxford University Press, New York, NY, USA, 1993.

[9] N. Friedman, M. Linial, I. Nachman, and D. Pe'er, "Using Bayesian networks to analyze expression data," *Journal of Computational Biology*, vol. 7, no. 3-4, pp. 601–620, 2000.

[10] H. De Jong, "Modeling and simulation of genetic regulatory systems: a literature review," *Journal of Computational Biology*, vol. 9, no. 1, pp. 67–103, 2002.

[11] I. Shmulevich, E. R. Dougherty, S. Kim, and W. Zhang, "Probabilistic Boolean networks: a rule-based uncertainty model for gene regulatory networks," *Bioinformatics*, vol. 18, no. 2, pp. 261–274, 2002.

[12] J. Goutsias and S. Kim, "A nonlinear discrete dynamical model for transcriptional regulation: construction and properties," *Biophysical Journal*, vol. 86, no. 4, pp. 1922–1945, 2004.

[13] S. Bornholdt, "Less is more in modeling large genetic networks," *Science*, vol. 310, no. 5747, pp. 449–451, 2005.

[14] P. T. Spellman, G. Sherlock, M. Q. Zhang, et al., "Comprehensive identification of cell cycle-regulated genes of the yeast Saccharomyces cerevisiae by microarray hybridization," *Molecular Biology of the Cell*, vol. 9, no. 12, pp. 3273–3297, 1998.

[15] J. J. Tyson, K. Chen, and B. Novak, "Network dynamics and cell physiology," *Nature Reviews Molecular Cell Biology*, vol. 2, no. 12, pp. 908–916, 2001.

[16] K. C. Chen, L. Calzone, A. Csikasz-Nagy, F. R. Cross, B. Novak, and J. J. Tyson, "Integrative analysis of cell cycle control in budding yeast," *Molecular Biology of the Cell*, vol. 15, no. 8, pp. 3841–3862, 2004.

[17] H. A. Armelin, J. Barrera, E. R. Dougherty, et al., "Simulator for gene expression networks," in *Microarrays: Optical Technologies and Informatics*, vol. 4266 of *Proceedings of SPIE*, pp. 248–259, San Jose, Calif, USA, January 2001.

[18] http://www.vision.ime.usp.br/~walter/pgn_cell_cycle/ycc_info.pdf.

[19] http://www.vision.ime.usp.br/~walter/pgn_cell_cycle/pgn_ccm_add_info.pdf.

[20] http://www.vision.ime.usp.br/~walter/pgn_cell_cycle/pgn_ccmrd_add_info.pdf.